Uncertainty propagation in aeolian processes: From threshold shear velocity to sand transport rate

(Article begins on next page)

04 August 2020

Uncertainty propagation in aeolian processes: from threshold shear velocity to sand transport rate

Lorenzo Raffaele[a,c,*], Luca Bruno[a,c], Giles F.S. Wiggs[b,c]

[a]*Politecnico di Torino, Department of Architecture and Design, Viale Mattioli 39, I-10125, Torino, Italy*
[b]*School of Geography and the Environment, Oxford University Centre for the Environment, University of Oxford, Oxford, OX1 3QY, UK*
[c]*Windblown Sand Modeling and Mitigation joint research group, Italy-France-UK*

Abstract

The accurate estimation of aeolian saltation events is a fundamental requirement in the modelling of wind erosion, dust emission, dune movement and aeolian hazard prediction. A large number of semi-empirical sand transport rate models exist, with many relying on a single value for a shear velocity threshold above which saltation is initiated. However, measuring and modelling the sand transport rate suffers from the effects of a number of epistemic and aleatory uncertainties which make the identification of a single threshold value for shear velocity problematic. This paper focuses on the uncertainty propagation evident in calculations that use a threshold shear velocity to estimate sand transport rate. Probability density functions of threshold shear velocity are provided from the authors' previous studies. Grain diameter and shear velocity are considered as deterministically varying parameters. Several sand transport rate statistical metrics are estimated via the Monte Carlo approach adopting four different sand transport models. The sand transport rate estimation in probabilistic terms allows us to assess the amplification/reduction in the uncertainty and to provide a deeper insight into established transport rate models. We find that if the wind speed is close to the erosion threshold, every tested model amplifies the variability of the resulting estimated sand transport rate, especially in the case of coarse sand. If the wind speed is large, the adopted models present substantial differences in uncertainty. An interpretation of these differences is given by conditioning the sand transport rate models to the type of erosion threshold adopted, the fluid or impact threshold.

Keywords: windblown sand saltation, sand transport rate, threshold shear velocity, uncertainty quantification

1. Introduction

The study of aeolian sand transport belongs to several research fields, from fundamental earth sciences to applied sciences such as civil and environmental engineering. From the scientific perspective, explaining and analysing wind-blown sand represents a challenging task due to the complex interactions between saltating particles, bed load and the wind field. Nevertheless, such analysis is an essential requirement in investigations of desert dust emissions (e.g. Haustein et al., 2015), dune dynamics (e.g. Wiggs and Weaver, 2012), agricultural wind erosion (e.g. Zobeck et al., 2003), land degradation (e.g. Mayaud et al., 2016), and planetary geomorphology (e.g. Kok et al., 2012). From the engineering perspective, windblown sand can have deleterious impacts on built structures and human activities (e.g. Zhang et al., 2010; Xie et al., 2015). For these reasons, the accurate prediction of sand transport events is a significant goal.

Saltation is the dominant mechanism of windblown sand transport. The total saltating load can be quantified by estimating the sand transport rate, i.e. by vertically integrating the horizontal flux of saltating particles. Since this physical quantity represents a straightforward measure to estimate wind erosion, sand transport, and deposition, a number of semi-empirical models to predict sand transport rate (Q-models) have been formulated (e.g. Kawamura,

---

*Corresponding author. Tel: (+39) 011.090.4870. Fax: (+39) 011.090.4999.
Email address: `lorenzo.raffaele@polito.it` (Lorenzo Raffaele)
URL: `http://www.polito.it/wsmm` (Lorenzo Raffaele)

1951; Owen, 1964; Lettau and Lettau, 1978; Kok et al., 2012).

Dong et al. (2003) classified sand transport models into four categories defined by their basic form. *Bagnold type* equations (e.g. Bagnold, 1941; Zingg, 1953) relate sand transport rate to the cube of shear velocity u_*^3 but do not explicitly consider the excess of shear velocity compared to a threshold value u_{*t}. This results in unrealistic sand transport rates when u_* is less than u_{*t}. *Modified Bagnold type* equations (e.g. Kawamura, 1951; Owen, 1964; Lettau and Lettau, 1978; Kok et al., 2012) relate sand transport rate to the cube of an effective shear velocity that is defined as a function of both the shear velocity and the threshold value. *O'Brien-Rindlaub type* and *modified O'Brien-Rindlaub type* equations (e.g. O'Brien and Rindlaub, 1936; Dong et al., 2003) relate transport rate to wind speed instead of shear velocity. These first three categories usually take into account the particle size directly through the sand grain diameter, d. The remaining models may be categorized as *complex*. These include physical models that account for additional phenomena in the saltation process such as inertial effects (Mayaud et al., 2017) or hysteresis (Kok, 2010). These models include multiple empirical fitting parameters usually related to quantities other than simply sand grain diameter.

Because of their ease of use and their sound physical basis, *modified Bagnold type* models are widespread in the literature and popularly employed in practice, see for example the field studies by Fryberger and Dean (1979), Al-Awadhi and Al-Awadhi (2009), Barchyn and Hugenholtz (2011), Sherman and Li (2012), Sherman et al. (2013), Yang et al. (2014) and Liu et al. (2015). However, *modified Bagnold type* models lead to significant variability in their prediction, despite belonging to the same conceptual form (e.g. Sarre, 1987; Sherman et al., 1998, 2013; Sherman and Li, 2012). These discrepancies follow from differences in the structure of models and can be related to the way the effective shear velocity and the grain diameter are treated in the model. For example, whilst some models explicitly account for changes in d (e.g. Lettau and Lettau, 1978), others do not (e.g. Kawamura, 1951), and still others account for the effect of d by introducing other related variables, such as the particle terminal velocity in the model of Owen (1964).

These differences can be regarded as the result of the inherent *uncertainty* in the saltation phenomenon. To our knowledge, a comprehensive description of uncertainties concerning the prediction of aeolian sand transport rate is not available in the literature. A useful approach is to consider a general classification of uncertainty in sand transport rate predictions that distinguishes between *aleatory* and *epistemic* uncertainty (Zio and Pedroni, 2013), both of which are relevant to the sand transport case.

Aleatory uncertainty refers to the inherent randomness in many physical phenomena (e.g. Sørensen, 1993). It arises not only in nature but also in the laboratory environment, where the properties of aeolian processes can be nominally controlled in both space and time.

Epistemic uncertainty is associated with the lack of knowledge about the properties and conditions of the phenomena to be modeled, i.e. *model*, *measurement* and *parameter* uncertainties (see Shao, 2008; Barchyn et al., 2014). We believe that the uncertainty concerning the mode of u_{*t} to be used in sand transport equations can be considered as an *epistemic model* uncertainty too because it is related to the lack of knowledge about the Q-model. Indeed, the mode of u_{*t} to be adopted is not unequivocally established in the literature. Two threshold velocities have been recognized: the fluid (or static) threshold, i.e. the minimum wind speed for initiation of sediment transport without antecedent transport; and the impact (or dynamic) threshold, i.e. the minimum wind speed for sustaining sediment transport with antecedent transport. There is no unanimity in the literature as to which threshold is the most appropriate for modelling sand transport rate: some authors prefer the impact threshold, others suggest the fluid threshold, and still others recommend a combination of the two. Pye and Tsoar (2009) and Kok et al. (2012) recommend the impact threshold defined as a linear function of the fluid threshold (85% and 80% of the fluid threshold, respectively). Similarly, Andreotti (2004) and Pahtz et al. (2012) also prefer the impact threshold and provide models for its estimation. Conversely, Shao (2008) refers to the fluid threshold only, whilst Sherman et al. (2013) adopt the fluid threshold for small Q and, for increasing Q, an exponential decreasing u_{*t} to a minimum equal to the impact threshold (85% of the fluid threshold). Kok (2010) provides a more sophisticated model for sand transport which considers a hysteretic threshold between the impact and fluid threshold that depends on the history of the system.

The uncertainties reviewed up to this point are innate in Q-models. We expect that the *uncertainty propagation* to Q from other models also occurs, also due to the uncertainty in u_{*t}. A few authors have recently raised this issue. Shao (2008) attributes the Q-model randomness not only to their empirical parameters but also to variability in the threshold shear velocity. Moreover, since a method to determine a single quantitative definition of u_{*t} is not agreed upon (see Stout, 2004), Shao (2008) notes that any estimate of u_{*t} must involve a degree of subjectivity. In particular,

he conjectured that such uncertainties in defining u_{*t} could outweigh the differences inherent in the functional forms of the sand transport rate models. The quantification of uncertainty in u_{*t} has recently been assessed by Raffaele et al. (2016), and Edwards and Namikas (2015) and Webb et al. (2016) note that such uncertainty in threshold estimates can be expected to propagate to sand transport rate predictions.

Given these points, two main questions are pertinent: i. How does the degree of uncertainty in sand transport rate (Q) vary with respect to the uncertainty in estimates for the threshold shear velocity (u_{*t})? ii. How do different sand transport rate models behave when threshold shear velocity is considered as a statistically random variable?

The present study aims to contribute to a solution to these issues. Four key, semi-empirical models of sand transport rate are adopted to evaluate the impact of uncertainty propagation. Threshold shear velocity is assumed as the only random variable affecting sand transport rate and, as a result, instead of having a single deterministic value of sand transport rate for given values of u_* and d, a range of different values describing a probability distribution are obtained.

2. Methods

Here we describe the method for evaluating uncertainty propagation from the parametric uncertainty of the threshold shear velocity to the model prediction of sand transport rate. First, the general approach is described and justified. Secondly, the adopted sand transport rate models and threshold shear velocity probability density functions are given. In this and following sections, the threshold shear velocity conditional probability density function $f(u_{*t} \mid d)$ is expressed as $f_{u_{*t}}$ for the sake of conciseness.

Uncertainty propagation from threshold shear velocity to predictions of sand transport rate is investigated by comparing dimensionless statistical metrics of both Q and u_{*t}. Both numerical and analytical solutions could be applied to evaluate uncertainty propagation (Smith, 2014). Analytically, for a given grain diameter and shear velocity, the cumulative distribution functions F_Q for sand transport rate can be obtained from the following procedure:

$$F_Q(s) = P[Q \leq s] = P[Q(u_{*t}) \leq s] = P\left[u_{*t} \leq Q^{-1}(s)\right] = F_{u_{*t}}\left[Q^{-1}(s)\right], \ \forall d, u_* \tag{1}$$

So, deriving each term, one can find the probability density functions f_Q:

$$f_Q(s) = f_{u_{*t}}\left[Q^{-1}(s)\right] \cdot \left[Q^{-1}(s)\right]', \ \forall d, u_* \tag{2}$$

It is worth noting from Equation 2 that the inversion of most of the sand transport rate models can only be performed numerically. Hence, we prefer a numerical approach because a fully analytical solution is not achievable. A classical Monte Carlo (MC) sampling based method (Caflisch, 1998) was preferred to other numerical approaches because of its very low computational cost. Furthermore, other numerical approaches (such as functional expansion-based methods like Karhunen-Loeve or polynomial chaos expansions) offer results that are too sophisticated for the relatively simple task covered by the present study. The MC method relies on repeated random sampling in order to obtain numerical probabilistic results. Hence, a set of numerical realizations of the random prediction $Q(u_*, u_{*t})$ was evaluated by varying $u_* \in [0.1, 2] \ m/s$ and by sampling the random parameter u_{*t} according to $f_{u_{*t}}$. In applying the MC method, it is important to check the convergence of the numerical realizations. Indeed, the rate of convergence of MC is always $1/n^{0.5}$, where n is the number of numerical realizations. It follows that the cardinality # of Q and u_{*t} affects the obtained results and must be chosen in order to reach the convergence of the first statistical moments of Q. Convergence can be checked by means of the weighted absolute error φ_{abs} as well as the weighted residual φ_{res} of the generic parameter φ. They are respectively defined for growing cardinality n as $\varphi_{abs} = |\varphi_{\#} - \varphi_n|/\varphi_{\#}$ and $\varphi_{res,n} = |\varphi_n - \varphi_{n-1}|/\varphi_n$.

In the framework of the MC method, sand transport rate is obtained by referring to some well-known modified Bagnold sand transport models reported in the literature. Semi-empirical modified Bagnold-type sand transport models proposed by Kawamura (1951), Owen (1964), Lettau and Lettau (1978) and Kok et al. (2012) were evaluated to assess the effects of uncertainty on transport predictions. These models are reported in Table 1, where ρ_a is the air density, g is the gravitational acceleration, d is the sand grain diameter, d_r is a reference sand grain diameter ($d_r = 0.25mm$) and K, O, L, C are semi-empirical parameters. For the model of Owen (1964), v_t is the particle's terminal velocity. Chen and Fryrear (2001) parametrized this as a function of the sand grain diameter getting

3

$v_t = -0.775352 + 4.52645d^{0.5}$, where v_t is expressed in m/s and d in mm.

Table 1: Summary of the adopted sand transport rate models

Reference	Equation	Semi-empirical parameter
Kawamura (1951)	$Q = K\frac{\rho_a}{g}u_*^3\left(1 - \frac{u_{*t}^2}{u_*^2}\right)\left(1 + \frac{u_{*t}}{u_*}\right)$	$K = 2.78$
Owen (1964)	$Q = O\frac{\rho_a}{g}u_*^3\left(1 - \frac{u_{*t}^2}{u_*^2}\right)$	$O = 0.25 + \frac{v_t}{3u_*}$
Lettau and Lettau (1978)	$Q = L\sqrt{\frac{d}{d_r}}\frac{\rho_a}{g}u_*^3\left(1 - \frac{u_{*t}}{u_*}\right)$	$L = 6.7$
Kok et al. (2012)	$Q = C\frac{\rho_a}{g}u_{*t}u_*^2\left(1 - \frac{u_{*t}^2}{u_*^2}\right)$	$C = 5$

It is worth stressing that the models proposed by Kawamura (1951) and Kok et al. (2012) do not explicitly take into account the grain diameter only because their semi-empirical parameter refers to $d \approx 0.25mm$. In this study their semi-empirical parameter is considered constant as an approximation. In fact, Kawamura (1951) does not define the relation between K and d, while Kok et al. (2012) provide a relation that cannot be easily computed. However, this assumption doesn't reflect on the uncertainty propagation to Q when expressed in dimensionless statistics such as coefficient of variation and skewness.

In this study, the fluid (or static) threshold shear velocity is adopted for several reasons. First, since it represents the starting point for erosion it is considered highly relevant for modelling purposes and application of model results. Secondly, unlike the impact threshold, appropriate probability density functions for the fluid threshold shear velocity are available from the literature (e.g. Duan et al., 2013; Raffaele et al., 2016). Thirdly, the fluid threshold is likely to be more variable than the impact threshold because it is more dependent upon variability in surface properties. Therefore, the analysis carried out in this paper will provide estimates of the maximum likely uncertainty propagation. Fourthly, when assuming the impact threshold as a linear function of the fluid threshold (i.e. $80\% - 85\%$ of the fluid threshold), the adoption of the fluid rather than the impact threshold doesn't affect the uncertainty propagation to Q when expressed in dimensionless statistics.

In order to account for the uncertainty in u_{*t}, conditional probability density functions of threshold shear velocity, $f_{u_{*t}}$ were taken from Raffaele et al. (2016). Given that u_{*t} varies as a function of d, one $f_{u_{*t}}$ exists for each value of d. We investigated a range of $d \in [0.063, 1.2]$ mm (i.e. from fine to coarse sand) by means of fifty linearly spaced non-parametric conditional probability density functions $f_{u_{*t}}$. Fig. 1 summarizes the statistics of the threshold shear velocity against d using suitable percentiles and statistical metrics. In Fig. 1(a), the trends of mean values $\mu(u_{*t})$ and the 1st, 5th, 25th, 75th, 95th and 99th percentiles p(u_{*t}) are plotted against the diameter d. In Fig. 1(b,c,d), the trends of the coefficient of variation $c.o.v.$, skewness sk and p$_{95}$/p$_{50}$ ratio are plotted, respectively.

3. Results

The section is organized as follows. Sub-section 3.1 provides preliminary results of the MC method. In Sub-section 3.2 the trend of the obtained statistical metrics is explored in order to clarify the complex graphs resulting from the three-dimensional surfaces of Q statistics.

3.1. Preliminary findings

First, we discuss the convergence of the first three Q statistical moments for an increasing cardinality n of $Q(u_*, u_{*t})$.
The weighted absolute error φ_{abs} as well as the weighted residual φ_{res} of the generic parameter φ were averaged over 100 random permutations of the order of $Q(u_*, u_{*t})$ for an assigned value of $u_*/\mu(u_{*t})$.
The rate of convergence is the same for each grain diameter, shear velocity and Q-model tested. However, the residuals differ with different Q-models and parameters. For example, in Fig. 2 the convergence of absolute and residual error is given with reference to the Kawamura (1951) model for $u_*/\mu(u_{*t}) = 1.5$ and $d = 0.25$ mm. Fig. 2(a) confirms that the rate of convergence of the absolute error clearly follows the slope $1/n^{0.5}$, in agreement with MC theory (Caflisch,
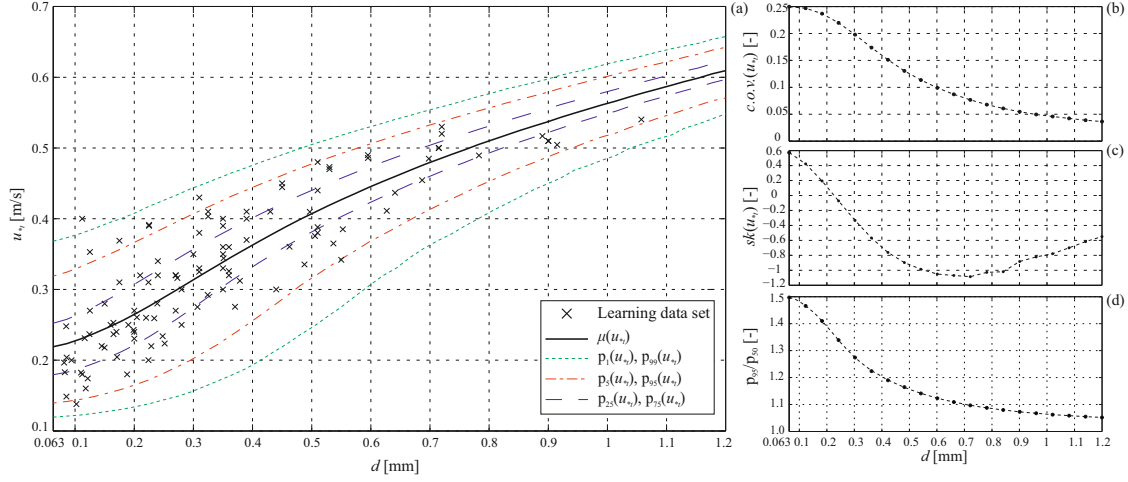
Figure 1: Threshold shear velocity statistics against d: mean values $\mu(u_{*t})$, $p_1(u_{*t})$, $p_5(u_{*t})$, $p_{25}(u_{*t})$, $p_{75}(u_{*t})$, $p_{95}(u_{*t})$, $p_{99}(u_{*t})$ percentiles (a). Coefficient of variation (b), skewness (c) and 95th percentile - 50th percentile ratio (d) of u_{*t}. Results derived from Raffaele et al. (2016)
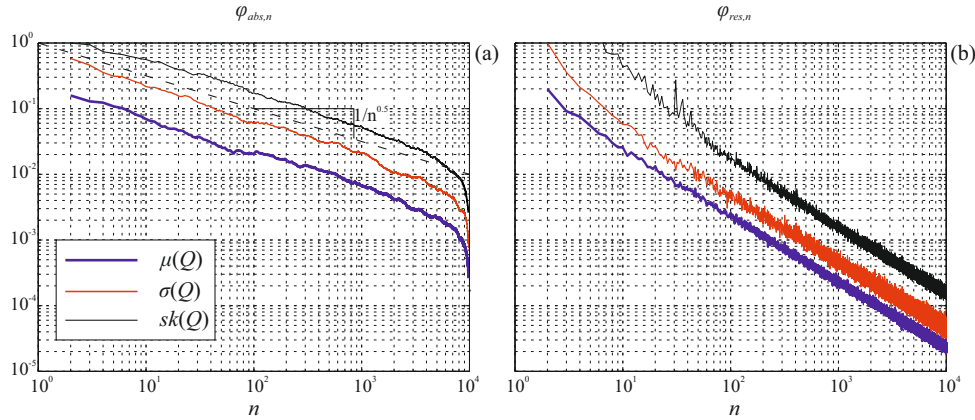

Figure 2: Assessment of the MC convergence: weighted absolute error (a) and weighted residual error (b) of the mean value μ, standard deviation σ and skewness sk of sand transport rate estimated by means of the Kawamura (1951) model for $d = 0.25$ mm and $u_*/\mu(u_{*t}) = 1.5$

1998). Fig. 2(b) plots the weighted residual to evaluate the total number of realizations # required to reach a desired accuracy. For the set-up above, even a modest cardinality $n = 5e+2$ allows $\mu_{res,n} \approx \sigma_{res,n} \approx 10^{-3}$ for the mean value and standard deviation of Q. This is a low residual error if compared with common engineering applications. As regards sk, $n = 2e+3$ allows a transport rate of about $sk_{res,n} \approx 10^{-3}$. Having in mind the low computational cost of a single realization and for the sake of precision, a cardinality # $= 1e+6$ is adopted in this study.

Overall, a probability density function of Q can be determined for each sand transport rate model and for each value of d and u_*. By way of example, two estimates of f_Q result from varying the Q-models, u_* and d are shown in Fig. 3(a),(b) and (c), respectively. The adopted $f_{u_{*t}}$ (dotted line) is also shown for each f_Q. The probability density functions are plotted over the normalized axis $\phi/p_{50}(\phi)$ of the generic variable ϕ. From Fig. 3, it is clear that different models, as well as different values of u_* and d, induce a significant variation in both variance and skewness of Q. As a result, the range of predicted values of Q also changes considerably. An increasing or decreasing variance with respect to the mean value of Q represents an amplification or reduction in the uncertainty, respectively. The skewness quantifies the degree of non-Gaussianity in that uncertainty.
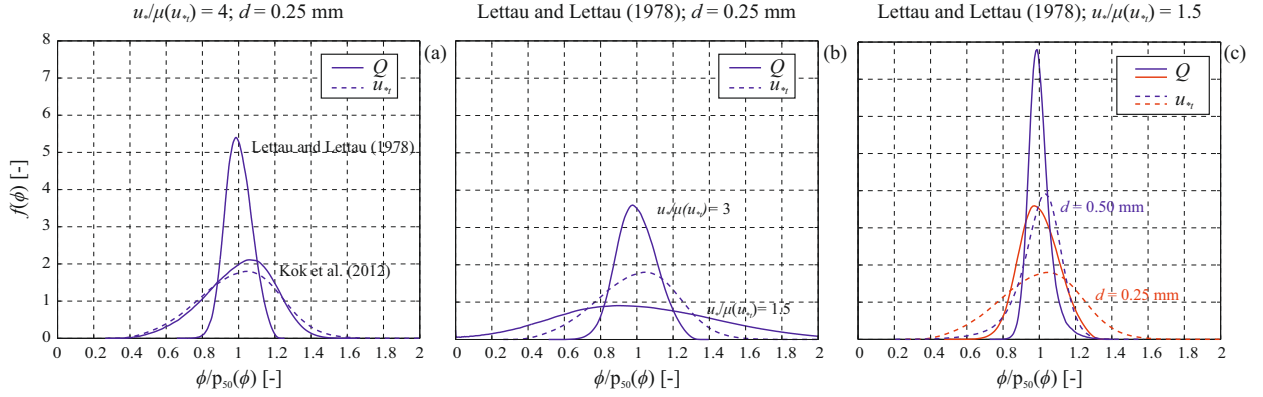
5

Figure 3: Comparison between normalized $f_{u_{*t}}$ and f_Q evaluated by varying Q-models (a), u_* (b) and d (c). The changes of both variance and skewness from $f_{u_{*t}}$ to f_Q are due to the uncertainty propagation.

3.2. Sensitivity analysis

For a given Q-model, a probability density function of Q corresponds to any point in the parameter plane $d - u_*$. In this study, this plane is sampled by 50 linearly spaced values of $d \in [0.063, 1.2]$ mm and 50 linearly spaced values of $u_* \in [0.1, 2]$ m/s. This results in as many as 2500 numerical estimates of f_Q for each Q-model, and in 10 billion realizations of Q in total. Given the considerable number of estimated densities f_Q, the uncertainty in sand transport rate is represented by means of its statistical moments, for the sake of brevity and clarity. The mean value μ, the 95th percentile p_{95}, the standard deviation σ and the skewness sk of Q $[kg\ m^{-1} s^{-1}]$ for each Q-model are plotted using contour plots in the parameter plane in Fig. 4.

Qualitatively, the results do not appear to differ significantly in average terms. The general trend of $\mu(Q)$ is the same for each sand transport model and also similar to $p_{95}(Q)$. $\mu(Q)$ monotonically increases with increasing u_* for a given d. Conversely, the trend over d for a given u_* is no more globally monotonic except for results from the Kawamura (1951) model. Here $\mu(Q)$ decreases with increasing d for small u_* even if the trend may be locally non-monotonic, while $\mu(Q)$ increases with increasing d for large u_*. Strong discrepancies between the models arise for higher order statistics $\sigma(Q)$ and $sk(Q)$, both qualitatively and quantitatively. However, some similarities in model behaviours can be recognized. First, results from Kawamura (1951) and Kok et al. (2012) are qualitatively similar (Fig. 4c,d and Fig. 4o,p, respectively). Indeed, both $\sigma(Q)$ and $sk(Q)$ show local maxima and minima. Secondly, high moments from Owen (1964) and Lettau and Lettau (1978) (Fig. 4g,h and Fig. 4k,l, respectively) reveal common trends. In particular, it is worth noting that $sk(Q)$ remains constant for increasing values of u_* above a common threshold of u_* for each grain size. In sum, while the model proposed by Owen (1964) behaves qualitatively like the one of Lettau and Lettau (1978), the model proposed by Kawamura (1951) behaves qualitatively like the one of Kok et al. (2012). Whilst some similarities can be identified in the qualitative general trend, the quantitative discrepancies remain significant.

In order to systematically discuss uncertainty propagation from u_{*t} to Q, Q statistics are compared to those of u_{*t}. We condense μ and σ into the coefficient of variation $c.o.v.$, and normalize p_{95} with respect to p_{50} in order to deal with dimensionless statistical metrics. In this way, metrics referring to u_{*t} can be directly compared with those of Q. For the sake of graphical clarity, the comparison is made by reducing the 3D plots in Fig. 4 to 2D plots, where the generic statistical metric φ is plotted versus one parameter for given values of the other.

In Fig. 5, $\varphi(Q)$ are plotted over d for each Q-model and for some sampled values of u_* (black continuous lines). The corresponding statistical metrics of u_{*t} versus d are plotted for comparison (dash dot lines). It is worth recalling that $\varphi(u_{*t})$ does not depend on u_* or the Q-model. Even if Q has a first order dependency on u_*, a stronger determinant is the effective shear velocity (Eq. 3), which takes into account the threshold value u_{*t}. Hence, in Fig. 5 the statistical metrics of Q are also plotted for given values of the averaged effective ratio $u_*/\mu(u_{*t})$ (dashed lines).

The variability of the sand transport rate over d with respect to its mean value, i.e. $c.o.v.(Q)$, is controlled by u_*
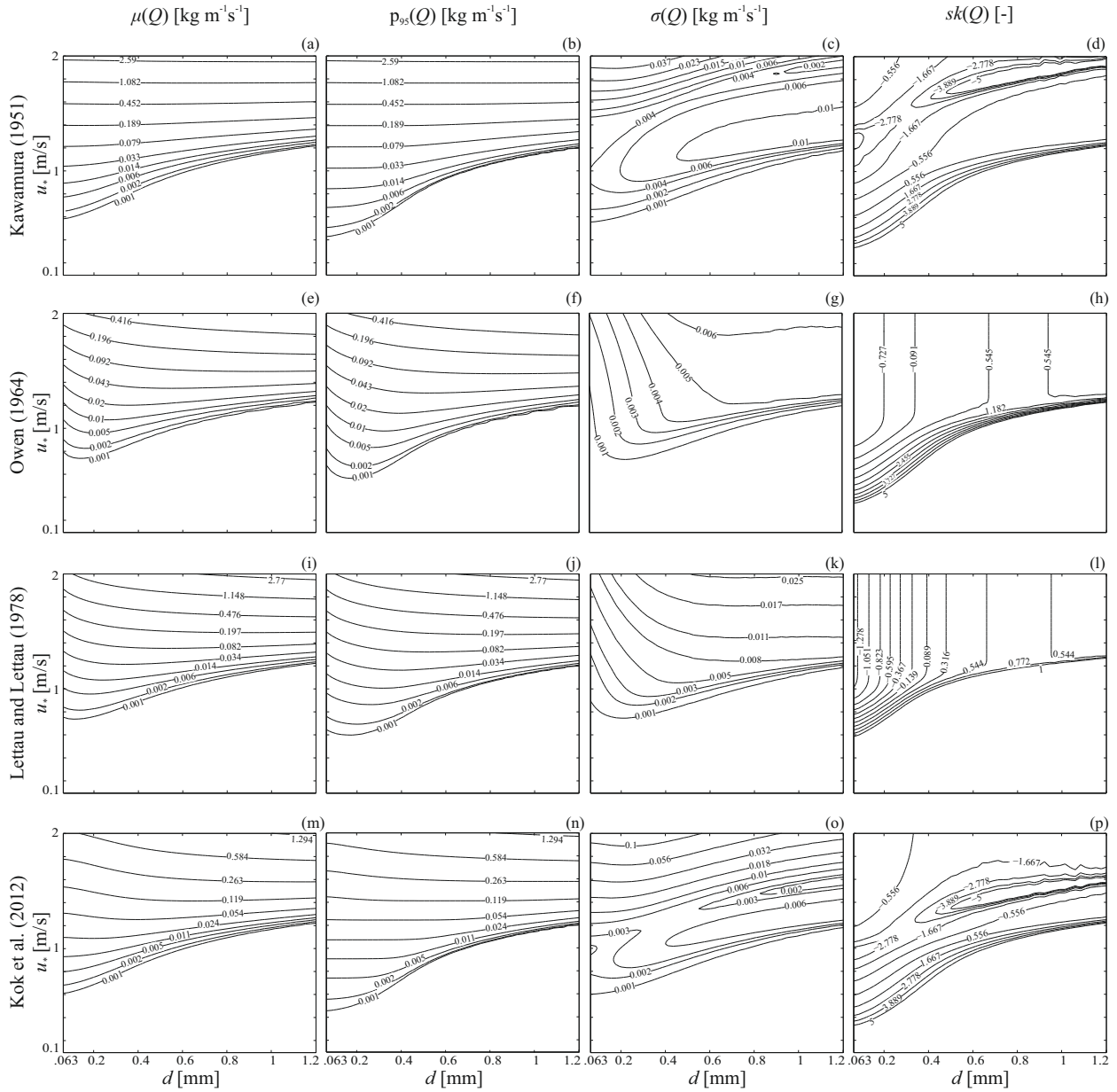
6

Figure 4: Contour plots of the first three statistical moments and 95th percentile of Q. Mean value μ, 95th percentile p_{95}, standard deviation σ and skewness sk according to different Q-models

(Fig. 5a,d). For slow winds (small u_*), the variability of Q is shown to increase with grain size for a given shear velocity for all the examined Q-models. For fast winds (large u_*), the results vary substantially depending on the Q-model. The influence of grain diameter on the variability of Q ($c.o.v.(Q)$) decreases considerably for the Owen (1964) and Lettau and Lettau (1978) models, while d strongly affects the variability of Q in the Kawamura (1951) and Kok et al. (2012) models. The $c.o.v.(Q)$ dependence on d is much clearer for fixed $u_*/\mu(u_{*t})$ ratios. Three fundamental states of the threshold shear velocity can be identified. First, when $u_* > \mu(u_{*t})$ the variability of Q decreases with increasing particle size, i.e. the low variability applies for coarse sands and large effective shear velocity. Secondly,
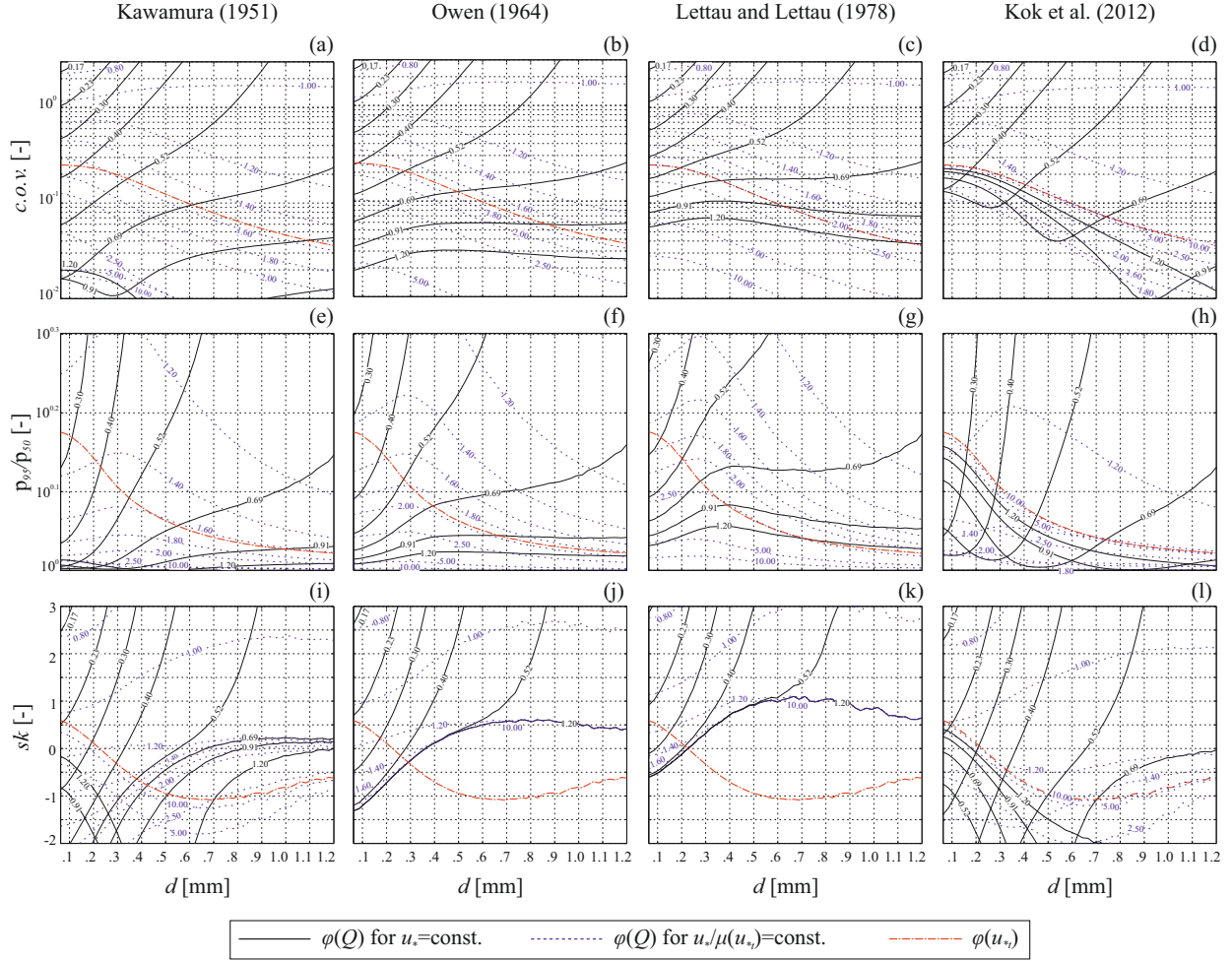
7

Figure 5: Uncertainty propagation from u_{*t} to Q. Q and u_{*t} statistical metrics versus d according to each Q-model

when $u_* \approx \mu(u_{*t})$ the variability of Q is not particularly affected by d. Thirdly, when $u_* < \mu(u_{*t})$ the variability increases with increasing grain diameter d. For a given value of d, the typical relationship is lower variability in Q at higher values of u_*, except in the case of the Kok et al. (2012) model (Fig. 5d).

The trend of $p_{95}/p_{50}(Q)$ versus d and u_* qualitatively follows the trend of $c.o.v.(Q)$ (Fig. 5e-h). Indeed, $p_{95}/p_{50}(Q)$ describes the variability of Q as a function of the tail event $p_{95}(Q)$, i.e. a large sand transport rate with a low chance of occurrence. Curves are simply stretched in the ordinate direction because $p_{95}/p_{50}(Q)$ address a characteristic variability rather than the standard variation as measured by $c.o.v.$. Analogously to $c.o.v.$, all the models approach $p_{95}/p_{50}(Q) = 1$ with increasing $u_*/\mu(u_{*t})$, except for the Kok et al. (2012) model where $p_{95}/p_{50}(Q)$ tends to $p_{95}/p_{50}(u_{*t})$.

Turning to the skewness (Fig. 5i-l), the behaviour of the models is qualitatively the same up to $u_* \approx 0.5\ m/s$: $sk(Q)$ increases over d, changing sign for $0.3 \le u_* \le 0.5$. Conversely, the trend of $sk(Q)$ over d for about $u_* > 0.5\ m/s$ varies significantly between the models and this is difficult to interpret. It is worth pointing out that $sk(Q)$ versus d for the Owen (1964) and Lettau and Lettau (1978) models does not vary for $u_* > 0.5\ m/s$. Conversely, $sk(Q)$ for the Kawamura (1951) and Kok et al. (2012) models changes its trend leading to local minima.

To better understand the behaviour of the models with varying u_*, statistical metrics are evaluated over $u_*/\mu(u_{*t})$ ratios for three fixed values of the sand grain diameter. In Fig. 6, $c.o.v.$, p_{95}/p_{50} and sk for Q are plotted over

8

$u_*/\mu(u_{*t}) \in [0.5, 50]$ at $d = \{0.1, 0.25, 0.5\}\, mm$. Values of u_* equal to fifty times the mean threshold shear velocity are out of scope for real world saltation phenomena. In fact, $u_* \approx 1 \div 2\, m/s$ for extreme winds and this equates to $u_*/\mu(u_{*t}) \approx 2 \div 10$ in Fig. 6. However, large u_* values are considered herein to assess the asymptotic behaviour of the statistical metrics. The values of the corresponding statistical metrics for u_{*t} are also reported for comparison.
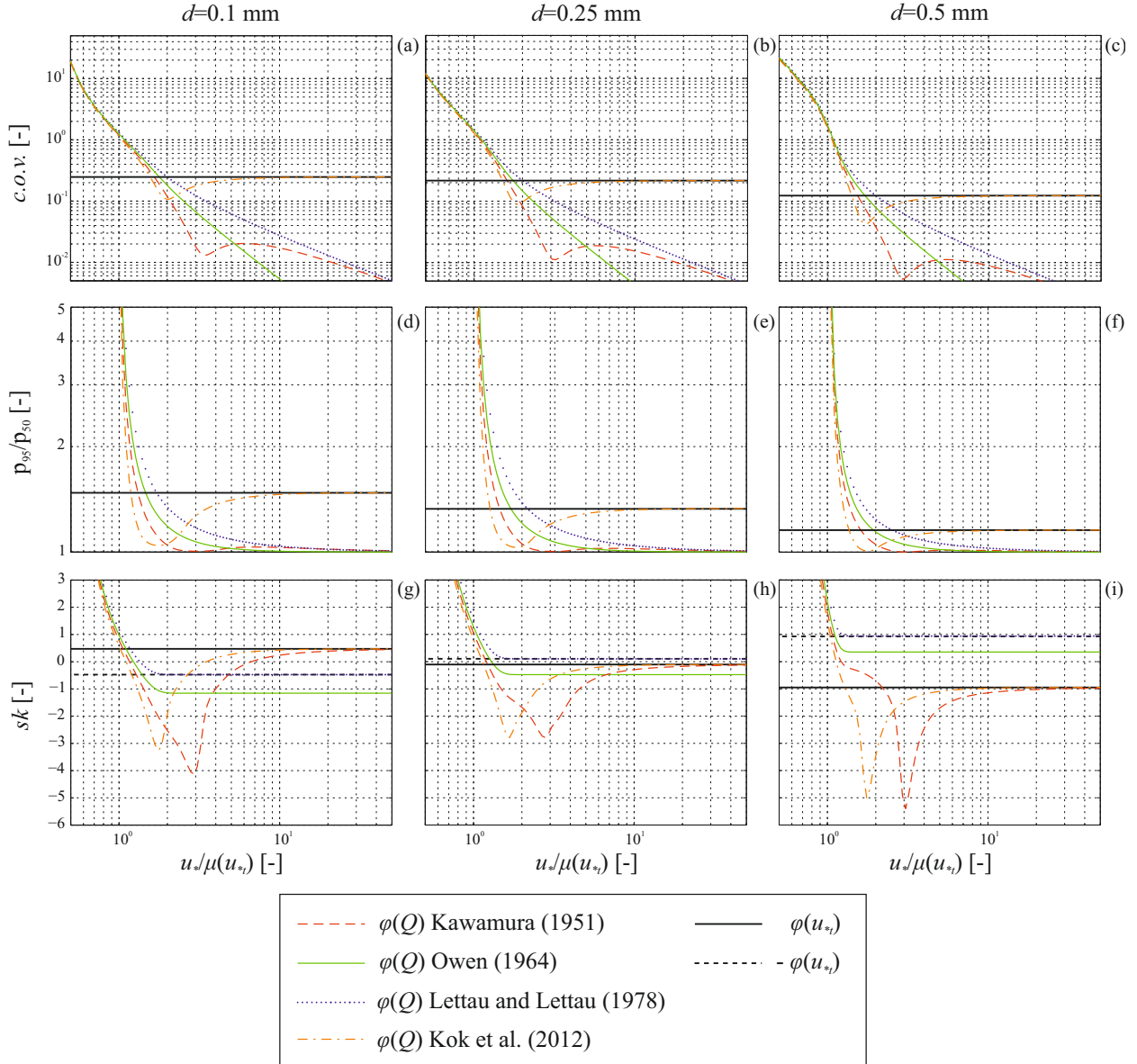

Figure 6: Uncertainty propagation from u_{*t} to Q. Q statistical metrics versus $u_*/\mu(u_{*t})$ ratio for each Q-model

Generally, all the Q-models show approximately the same trend for all statistical metrics up to $u_*/\mu(u_{*t}) \approx 1$ (i.e. small or null Q). Conversely, each model shows a different behaviour at larger ratios at higher wind speeds. Hence, the uncertainty will propagate differently for $u_*/\mu(u_{*t}) > 1$. $c.o.v.(Q)$ and $p_{95}/p_{50}(Q)$ (Fig. 6a-f) provide a reasonable measure of the variability of Q, and some information on the uncertainty propagation from u_{*t} to Q, i.e. if variability is damped or amplified. Focusing on $c.o.v.(Q)$, the uncertainty in u_{*t} is amplified where $u_*/\mu(u_{*t}) < 1.5$. Conversely,

9

the uncertainty is damped where $u_*/\mu(u_{*t}) > 1.5$, except in the case of the Kok et al. (2012) model. In the case of $u_*/\mu(u_{*t}) > 1.5$, the variability resulting from the Owen (1964) and Lettau and Lettau (1978) models decreases and tends monotonically to zero, while the variability resulting from the Kawamura (1951) and Kok et al. (2012) models exhibit local minima before tending to the curve of Lettau and Lettau (1978) and $c.o.v.(u_{*t})$, respectively. The model that shows the fastest convergence rate to zero is the one proposed by Owen (1964). The trend of $p_{95}/p_{50}(Q)$ highlights once again that the variability in Q decreases for increasing values of u_*, except for data derived from the model of Kok et al. (2012).

The skewness values (Fig. 6g-i) better highlight the different behaviour of each model against $u_*/\mu(u_{*t})$. In general, the sand transport rate predictions are non-Gaussian. For small $u_*/\mu(u_{*t})$, they are all highly positively skewed. Indeed, f_Q will show an extremely large frequency of null transport (i.e. a peak for $Q = 0$) and very low frequencies of non-null transport (i.e. right-tailed distribution). For intermediate $u_*/\mu(u_{*t})$, the results from the Kawamura (1951) and Kok et al. (2012) models are highly negatively skewed, while the skewness from the Lettau and Lettau (1978) and Owen (1964) models is related to $sk(u_{*t})$. For large $u_*/\mu(u_{*t})$, the degree of non-Gaussianity decreases to values related to $sk(u_{*t})$.

The above results are determined by MC-based numerical experiments. The non-trivial trends observed suggest there is value in interpreting them in analytical terms by basic a-posteriori uncertainty propagation analysis. In order to do so, we generalized the adopted modified Bagnold type models to the same basic form:

$$Q = \Phi \, \frac{\rho_a}{g} \, u_{*,eff}^3 \, (u_*, u_{*t}) \tag{3}$$

where Φ is the dimensionless semi-empirical parameter and $u_{*,eff}^3$ is the effective shear velocity determined as a function of u_* and u_{*t}. The expressions of $u_{*,eff}^3$ is given in the second column of Table 2, for each Q-model. In deterministic terms, $u_{*,eff}^3$ is a third order polynomial of the variables u_* and u_{*t}. Although, the analytical study of the function $u_{*,eff}^3$ is feasible, it is out of scope of the present study. In probabilistic terms, $u_{*,eff}^3$ is a transformation of the random variable u_{*t} and a function of the deterministic variable u_*. The analytical study of the statistical metrics of Q is unfeasible, since uncertainty propagation depends on the combination of u_* and u_{*t} in a non-trivial way. Some light can be shed by the analytical evaluation of the limits of the statistical metrics of Q for $u_* \to +\infty$. Given Equation 3, the limit of Q metrics is equivalent to the one of $u_{*,eff}^3(u_*, u_{*t})$. The limits of $c.o.v.(Q)$, $sk(Q)$ and $p_{95}/p_{50}(Q)$ are obtained having in mind the basic properties of the same statistical metrics. For example, by referring to the $c.o.v.(Q)$ resulting from the Kok et al. (2012) model we have:

$$\lim_{u_* \to +\infty} c.o.v.(Q) = \lim_{u_* \to +\infty} \frac{\sigma(Q)}{\mu(Q)} = \lim_{u_* \to +\infty} \frac{\sigma\left(u_{*,eff}^3\right)}{\mu\left(u_{*,eff}^3\right)} = \lim_{u_* \to +\infty} \frac{u_*^2 \sigma(u_{*t})}{u_*^2 \mu(u_{*t})} = \frac{\sigma(u_{*t})}{\mu(u_{*t})} = c.o.v.(u_{*t}) \tag{4}$$

Conversely, by referring to the $c.o.v.(Q)$ resulting from all the other models:

$$\lim_{u_* \to +\infty} c.o.v.(Q) = \lim_{u_* \to +\infty} \frac{\sigma(Q)}{\mu(Q)} = \lim_{u_* \to +\infty} \frac{\sigma\left(u_{*,eff}^3\right)}{\mu\left(u_{*,eff}^3\right)} = \lim_{u_* \to +\infty} \frac{\sigma\left(u_*^3\right)}{\mu\left(u_*^3\right)} = 0 \tag{5}$$

Table 2 reports the full list of the analytical limits for each Q-model and statistical metric. In particular, they confirm the right-sided asymptotic tendencies of Fig. 6.

Previously, we explored the asymptotic behaviour of the statistical metrics of Q. However, the limits for $u_* \to +\infty$ are not relevant in the practice. Hence, we reduced the range of the shear velocity under investigation so to assess realistic values of the coefficient of variation. In doing this we set the roughness length $z_0 = 0.003 \, m$ and the interval $u_* \in [0.1, 1] \, m/s$. Such an interval corresponds to approximate wind speed values between 2 (light breeze) and 8 (gale) on the Beaufort scale, i.e. a scale that relates wind speed to observed weather conditions (Hasse, 2015). Furthermore, we adopted an additional condition on the mean value of Q in order to discard very large $c.o.v.$ which correspond to very low sand transport rates. Hence, values of $\mu(Q) \geq 10^{-3} kg \, m^{-1} s^{-1}$ are used in the analysis. The resulting values of the ratio $c.o.v.(Q)/c.o.v.(u_{*t})$ are reported in Fig. 7 for each model, and for three values of the sand grain diameter, namely $d \in \{0.1, 0.25, 0.50\} \, mm$.

Table 2: Limits of dimensionless statistical metrics of Q for $u_* \to +\infty$

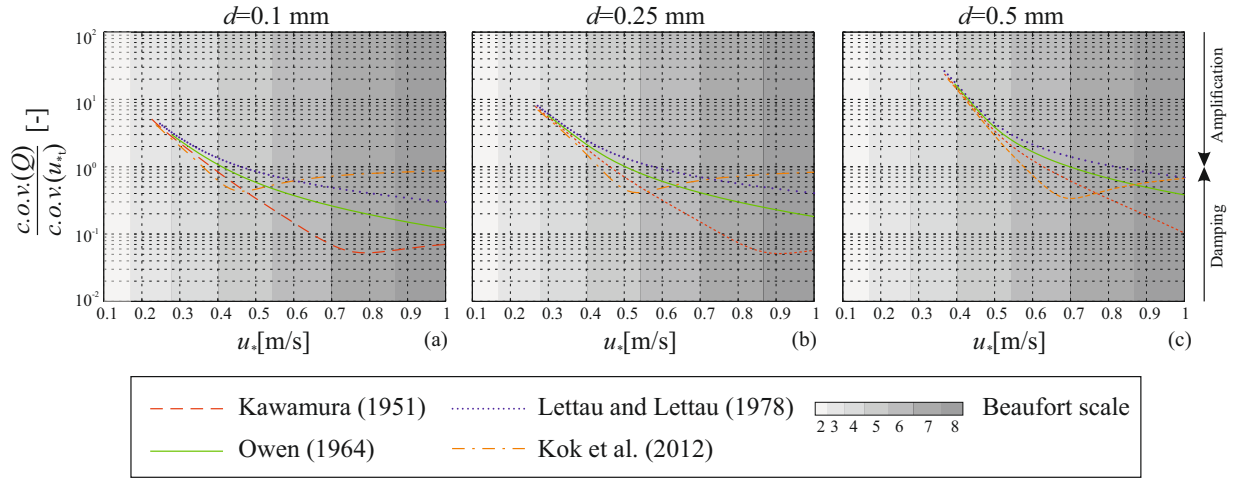| Reference	$u_{*,eff}^3 (u_*, u_{*t})$	$\lim_{u_* \to +\infty} c.o.v.(Q)$	$\lim_{u_* \to +\infty} p_{95}/p_{50}(Q)$	$\lim_{u_* \to +\infty} sk(Q)$
Kawamura (1951)	$u_*^3 \left(1 - \frac{u_{*t}^2}{u_*^2}\right)\left(1 + \frac{u_{*t}}{u_*}\right)$	0	0	$sk(u_{*t})$
Owen (1964)	$u_*^3 \left(1 - \frac{u_{*t}^2}{u_*^2}\right)$	0	0	$-sk(u_{*t}^2)$
Lettau and Lettau (1978)	$u_*^3 \left(1 - \frac{u_{*t}}{u_*}\right)$	0	0	$-sk(u_{*t})$
Kok et al. (2012)	$u_*^2 u_{*t} \left(1 - \frac{u_{*t}^2}{u_*^2}\right)$	$c.o.v.(u_{*t})$	$p_{95}/p_{50}(u_{*t})$	$sk(u_{*t})$

Figure 7: Uncertainty propagation from u_{*t} to Q for realistic values of u_*. $c.o.v.(Q)/c.o.v.(u_{*t})$ versus $u_*/\mu(u_{*t})$ for each Q-model and $u_* \in [0.1, 1] \, m/s$

Fig. 7 quantifies the actual magnitude of the uncertainty propagation. In particular, $c.o.v.(Q)/c.o.v.(u_{*t}) > 1$ reflects uncertainty amplification, while $c.o.v.(Q)/c.o.v.(u_{*t}) < 1$ reflects uncertainty damping. Generally, $c.o.v.(Q)/c.o.v.(u_{*t})$ covers a range from 1 to 2 orders of magnitude. The variability in Q changes significantly in the adopted range of wind speed, ranging from small values below unity for gales (damped uncertainty from u_{*t} to Q) to very high values above unity and up to 20 for breezes (amplified uncertainty), notably for coarser sands. Indeed, $c.o.v.(Q)/c.o.v.(u_{*t})$ increases with increasing d for small values of $u_*/\mu(u_{*t})$. Conversely, $c.o.v.(Q)/c.o.v.(u_{*t})$ remains almost constant with increasing d for large values of $u_*/\mu(u_{*t})$. Hence, the variation in particle size mostly affects the uncertainty propagation when u_* is close to $\mu(u_{*t})$.

4. Discussion

Our results indicate that the uncertainty in threshold shear velocity u_{*t} propagates into predictions of sand transport rate Q. The numerical uncertainty propagation investigated in this study can be viewed as a reflection of both *physical* and *statistical* processes. From a physical point of view, the variability of u_{*t} affects the mechanics of the sand saltation. From a statistical point of view, the modelling, measurement, and parametric uncertainty in u_{*t} propagates to Q. However, the characteristics of this propagation vary depending upon the Q-model, the sand grain diameter d, and the wind shear velocity u_*.

The discrepancies in uncertainty propagation among Q-models can be ascribed to the general form of $u_{*,eff}^3$. For the sake of clarity, the effective shear velocity was split between $u_{*,eff}^3 = \mathcal{U}_* \Psi_*$, where $\mathcal{U}_*$ representing *sustained saltation* and Ψ_* representing *triggering of saltation*. In particular, $\mathcal{U}_*$ express the scaling of the particle speed, while

11

Ψ_* express the effective shear velocity translation as a function of u_{*t}. The resulting values of $\mathcal{U}_*$ and Ψ_* for each Q-model are reported in Table 3.

Table 3: General form of the effective shear velocity $u_{*,eff}^3 = \mathcal{U}_* \Psi_*$. Saltation sustaining $\mathcal{U}_*$ and saltation triggering Ψ_* according to each sand transport rate model

Reference	$\mathcal{U}_*$	Ψ_*
Kawamura (1951)	$u_* + u_{*t}$	$u_*^2 - u_{*t}^2$
Owen (1964)	u_*	$u_*^2 - u_{*t}^2$
Lettau and Lettau (1978)	u_*^2	$u_* - u_{*t}$
Kok et al. (2012)	u_{*t}	$u_*^2 - u_{*t}^2$

The physical interpretation of our results is clear from Table 3. The Kok et al. (2012) model propagates the same amount of uncertainty of u_{*t} to Q for strong winds. In formulas, for the generic dimensionless statistical metric φ, it holds that $\lim_{u_* \to +\infty} \varphi(Q) = \varphi(u_{*t})$. Conversely, the other models behave differently: the uncertainty is damped from u_{*t} to Q for strong winds and the variation tends to zero. An interpretation of these marked differences in behaviour of the models can be obtained with reference to the saltation sustaining $\mathcal{U}_*$ and the saltation triggering Ψ_*.

$\mathcal{U}_*$ drives the uncertainty propagation for strong winds since $\lim_{u_* \to +\infty} \varphi(\Psi_*) = 0$. Kok et al. (2012) explicitly adopt the impact threshold for $\mathcal{U}_*$. Under this assumption the asymptotic trend of Q statistical metrics looks physically sound since saltation is carried out by grain impacts and the particle terminal velocity does not depend on u_* (see Kok et al., 2012, and related references). Owen (1964) and Lettau and Lettau (1978) adopt u_* and u_*^2, respectively. Hence, saltation is sustained purely by wind entrainment. Kawamura (1951) adopts the sum of u_* and u_{*t}. However, the statistical metrics of the Kawamura (1951) model tend to the ones of Owen (1964) and Lettau and Lettau (1978) for strong winds. In this sense, the models of Kawamura (1951), Owen (1964) and Lettau and Lettau (1978) are consistent with the adoption of the fluid threshold. Under this assumption saltation is initiated purely by wind entrainment and uncertainty in the fluid threshold has a greater impact at wind speeds close to the threshold. This issue represents a source of epistemic model uncertainty since uncertainty in threshold choice is not a resolved debate in the scientific literature. We hope that the present study contributes to the discussion on this open issue and stimulates debate. It is worth pointing out that the effective shear velocity in Kawamura (1951) is the summation of the $u_{*,eff}^3$ from Owen (1964) and Kok et al. (2012). Indeed, the statistical metrics of Q resulting from the Kawamura (1951) model are hybrid (see Fig. 6).

As regards Ψ_*, it is the same for all the Q-models except for Lettau and Lettau (1978). Indeed, for the Kawamura (1951), Owen (1964) and Kok et al. (2012) models Ψ_* reflects the general physical scaling $Q \propto \tau_{eff} = \rho_a(u_*^2 - u_{*t}^2)$, where τ_{eff} is the effective shear stress. Conversely, the Lettau and Lettau (1978) model shows a linear translation. We believe that the reasons for this discrepancy could be ascribed to the empirical fitting of the Q-model.

In light of our results, three main observations can be made:

1. Differences in the propagation of uncertainty between different sand transport models are significant and can reach an order of magnitude. Sarre (1987), Sherman et al. (1998, 2013) and Sherman and Li (2012) have highlighted the discrepancies between models in deterministic terms. The adoption of one model over another gives rise to differences not only in the mean values, but also much larger differences in terms of variance, skewness and extreme percentiles (see Fig. 4). These kinds of discrepancies between model predictions become more noticeable in the range $u_*/\mu(u_{*t}) \in [2, 5]$ (see Fig. 6). This range is of practical interest for real world windblown sand events;

2. Differences in uncertainty propagation caused by varying u_* show that for slow wind speeds the uncertainty in Q is amplified with respect to the uncertainty in u_{*t}. Slow wind speeds occur frequently in nature due to the Weibull probability density function of wind speed. Hence, amplification in Q uncertainty is a potentially large practical issue if not accounted for correctly. In contrast, in strong winds the uncertainty of u_{*t} does not significantly affect Q, except in the model results of Kok et al. (2012) (see Fig. 6a-c). The physical interpretation of the local and global minima of the statistical metrics occurring for intermediate values of $u_*/\mu(u_{*t}) \in [2, 3]$ in Kawamura (1951) and Kok et al. (2012) is not straightforward (Fig. 6). Analytically, they result from the

presence of u_{*t} in the saltation sustaining term $\mathcal{U}_*$. In the practice, the global minima of the skewness imply an underestimation of Q for related wind speeds by employing the Kawamura (1951) and Kok et al. (2012) models with respect to the Owen (1964) and Lettau and Lettau (1978) models;

3. Differences in uncertainty propagation caused by varying the sand grain diameter, d, highlight that, for slow winds the variability in Q increases for coarse sands whilst, for strong winds, the variability in Q is less affected by d, except in the model results of Kok et al. (2012) (see Fig. 5a-d). For realistic values of u_*, errors in the estimation of d propagate to Q prediction primarily for slow winds (Fig. 7). However, it is worth pointing out that the effect of d on the nominal sand transport rate remains an open issue (Dong et al., 2003; Valence, 2015).

In light of the above observations, the choice of a Q-model should be performed not only to achieve the best prediction of the mean sand transport rate, but also in consideration of the uncertainty propagation in practical estimation of probabilistic sand transport rate. However, care must be taken since the choice of the model considerably affects the uncertainty of Q predictions. Further experimental investigations on sand transport rate uncertainty could shed some light on these issues.

5. Conclusions

The present study critically investigated the uncertainty propagation from threshold shear velocity to sand transport rate. In particular, threshold shear velocity was considered as the only source of randomness in sand transport rate models, while the other parameters were assumed to be deterministic. Statistical moments and metrics of Q were assessed via the Monte Carlo method by varying the adopted sand transport model and the values of u_* and d.

Our results have allowed us to assess the amplification or reduction in the uncertainty of sand transport rate with respect to the uncertainty in threshold shear velocity. The strong differences in uncertainty propagation between examined sand transport rate models led us to ascribe them to the general form of the effective shear velocity. In particular, in the case of slow speed winds close to the erosion threshold, every model we have tested tends to amplify the variability of Q, in some cases up to 20 times the variability of u_{*t}. In addition, the variability of Q is seen to increase for coarse sand. These results allow further insight into the behaviour of the sand transport rate models. In the case of strong winds, Q-models present two substantial differences. The models of Kawamura (1951); Owen (1964); Lettau and Lettau (1978) dampen the uncertainty in u_{*t} and the effect of d on Q uncertainty, while the model of Kok et al. (2012) propagates the exact amount of uncertainty in u_{*t} to Q. The adoption of a particular sand transport model therefore has implications not only on the mean value of Q but also on Q uncertainty.

In light of these results, we highlight three research opportunities:

First, considering the large discrepancies in statistical terms between different models belonging to the same basic form of *modified Bagnold type* models, it would be worth assessing by means of experimental measurements how the uncertainty physically propagates from u_{*t} to Q.

Second, the development of a generalized probabilistic model for sand transport rate would be worth further investigation.

Third, since our results refer to the uncertainty evident in the instantaneous sand transport rate, it might be worth investigating how the uncertainty propagates when evaluating the drift potential (DP), i.e. the cumulative value of the sand transport rate over time (Fryberger and Dean, 1979). We conjecture that the uncertainty in DP will be damped. Indeed, the sum of independent and identically distributed random variables is expected from theory to reduce the resultant coefficient of variation. However, the entity of the uncertainty in DP should be quantified and, if significant, considered in practice.

References

Al-Awadhi, J.M., Al-Awadhi, A.A., 2009. Modeling the aeolian sand transport for the desert of Kuwait: Constraints by field observations. Journal of Arid Environments 73, 987–995. doi:10.1016/j.jaridenv.2009.04.023.

Andreotti, B., 2004. A two-species model of aeolian sand transport. Journal of Fluid Mechanics 510, 47–70. doi:10.1017/S0022112004009073.

Bagnold, R.A., 1941. The Physics of Blown Sand and Desert Dunes. Dover Earth Science.

Barchyn, T.E., Hugenholtz, C.H., 2011. Comparison of four methods to calculate aeolian sediment transport threshold from field data: Implications for transport prediction and discussion of method evolution. Geomorphology 129, 190–203. doi:10.1016/j.geomorph.2011.01.022.

Barchyn, T.E., Martin, R.L., Kok, J.F., Hugenholtz, C.H., 2014. Fundamental mismatches between measurements and models in aeolian sediment transport prediction: The role of small-scale variability. Aeolian Research 15, 245–251. doi:10.1016/j.aeolia.2014.07.002.

Caflisch, R., 1998. Monte carlo and quasi-monte carlo methods. Acta Numerica 7, 1–49. doi:10.1017/S0962492900002804.

Chen, W., Fryrear, D.W., 2001. Aerodynamic and geometric diameter of airborne particles. Journal of Sedimentary Research 71, 365–371. doi:10.1306/2DC4094A-0E47-11D7-8643000102C1865.

Dong, Z., Liu, X., Wang, H., Wang, X., 2003. Aeolian sand transport: a wind tunnel model. Sediment. Geol. 161, 71–83. doi:10.1016/S0037-0738(03)00396-2.

Duan, S., Cheng, N., Xie, L., 2013. A new statistical model for threshold friction velocity of sand particle motion. Catena 104, 32–38. doi:10.1016/j.catena.2012.04.009.

Edwards, B.L., Namikas, S.L., 2015. Characterizing the sediment bed in terms of resistance to motion: Toward an improved model of saltation thresholds for aeolian transport. Aeolian Research 19, 123–128. doi:10.1016/j.aeolia.2015.10.004.

Fryberger, S., Dean, G., 1979. A Study of Global Sand Seas. chapter Dune forms and wind regime. pp. 137–155.

Hasse, L., 2015. Encyclopedia of Atmospheric Sciences (Second Edition). chapter BASIC ATMOSPHERIC STRUCTURE AND CONCEPTS — Beaufort Wind Scale. pp. 1–6.

Haustein, K., Washington, R., King, J., Wiggs, G., Thomas, D.S.G., Eckardt, F.D., Bryant, R.G., Menut, L., 2015. Testing the performance of state-of-the-art dust emission schemes using do4models field data. Geosci. Model Dev 8. doi:10.5194/gmd-8-341-2015.

Kawamura, R., 1951. Study of sand movement by wind. Technical Report. NASA technical translation.

Kok, J.F., 2010. Difference in the wind speeds required for initiation versus continuation of sand transport on mars: Implications for dunes and dust storms. Physical Review Letters 104. doi:10.1103/PhysRevLett.104.074502.

Kok, J.F., Parteli, E.J.R., Michaels, T.I., Karam, D.B., 2012. The physics of wind-blown sand and dust. Reports on Progress in Physics 75, 106901. doi:10.1088/0034-4885/75/10/106901.

Lettau, K., Lettau, H., 1978. Experimental and micro-meteorological field studies of dune migration. Technical Report 101, 110-147. Exploring the Worlds Driest Climate (IES Report, 101, 110147).

Liu, L., Yang, Y., Shi, P., Zhang, G., Qu, Z., 2015. The role of maximum wind speed in sand-transporting events. Geomorphology 238, 177–186. doi:10.1016/j.geomorph.2015.03.007.

Mayaud, J.R., Bailey, R.M., Wiggs, G.F.S., Weaver, C.M., 2017. Modelling aeolian sand transport using a dynamic mass balancing approach. Geomorphology 280, 108–121. doi:10.1016/j.geomorph.2016.12.006.

Mayaud, J.R., Wiggs, G.F., Bailey, R.M., 2016. Measurement and data analysis methods for field-scale wind erosion studies and model validation. Earth Surface Processes and Landforms. doi:10.1002/esp.4082. eSP-16-0229.R1.

O'Brien, M., Rindlaub, B., 1936. The transportation of sand by wind. Civil Engineering 6, 325–327.

Owen, P.R., 1964. Saltation of uniform grains in air. Journal of Fluid Mechanics 20, 225–242. doi:10.1017/S0022112064001173.

Pahtz, T., Kok, J.F., Herrmann, H.J., 2012. The apparent roughness of a sand surface blown by wind from an analytical model of saltation. New Journal of Physics 14. doi:10.1088/1367-2630/14/4/043035.

Pye, K., Tsoar, H., 2009. Aeolian Sand and Sand Dunes. Springer. doi:10.1007/978-3-540-85910-9.

Raffaele, L., Bruno, L., Pellerey, F., Preziosi, L., 2016. Windblown sand saltation: A statistical approach to fluid threshold shear velocity. Aeolian Research 23, 79–91. doi:10.1016/j.aeolia.2016.10.002.

Sarre, R.D., 1987. Aeolian sand transport. Progress in Physical Geography 11, 157–182. doi:10.1177/030913338701100201.

Shao, Y., 2008. Physics and Modelling of Wind Erosion. Springer. doi:10.1007/978-1-4020-8895-7.

Sherman, D.J., Bailiang, L., Ellis, J.T., Farrell, E.J., Maia, L., Granja, H., 2013. Recalibrating aeolian sand transport models. Earth Surf. Process. Landforms 38, 169–178. doi:10.1002/esp.3310.

Sherman, D.J., Jackson, D.W.T., Namikas, S.L., Wang, J., 1998. Wind-blown sand on beaches: an evaluation of models. Geomorphology 22, 113–133. doi:10.1016/S0169-555X(97)00062-7.

Sherman, D.J., Li, B., 2012. Predicting aeolian sand transport rates: A reevaluation of models. Aeolian Research 3, 371–378. doi:10.1016/j.aeolia.2011.06.002.

Smith, R., 2014. Uncertainty Quantification: Theory, Implementation, and Applications. Society for Industrial and Applied Mathematics, Philadelphia, PA, USA.

Sørensen, M., 1993. Stochastic models of sand transport by wind and two related estimation problems. International Statistical Review 61, 245–255. doi:10.2307/1403627.

Stout, J.E., 2004. A method for establishing the critical threshold for aeolian transport in the field. Earth Surface Processes and Landforms 29, 1195–1207. doi:10.1002/esp.1079.

Valence, A and Rasmussen, K R and El Moctar, A O and Dupont, P, 2015. The physics of Aeolian sand transport. Comptes Rendus Physique 16, 105–117. doi:110.1016/j.crhy.2015.01.006.

Webb, N.P., Galloza, M.S., Zobeck, T.M., Herrick, J.E., 2016. Threshold wind velocity dynamics as a driver of aeolian sediment mass flux. Aeolian Research 20, 45 – 58. doi:10.1016/j.aeolia.2015.11.006.

Wiggs, G.F.S., Weaver, C.M., 2012. Turbulent flow structures and aeolian sediment transport over a barchan sand dune. Geophysical Research Letters 39. doi:10.1029/2012GL050847. l05404.

Xie, L.W., Zhong, J., Chen, F.F., Cao, F.X., Li, J.J., Wu, L.C., 2015. Evaluation of soil fertility in the succession of karst rocky desertification using principal component analysis. Solid Earth 6, 515–524. doi:10.5194/se-6-515-2015.

Yang, Y., Qu, Z., Shi, P., Liu, L., Zhang, G., Tang, Y., Hu, X., Lv, Y., Xiong, Y., Wang, J., Shen, L., Lv, L., Sun, S., 2014. Wind regime and sand transport in the corridor between the badain jaran and tengger deserts, central alxa plateau, china. Aeolian Research 12, 143–156. doi:10.1016/j.aeolia.2013.12.006.

Zhang, K., Qu, J., Liao, K., Niu, Q., Han, Q., 2010. Damage by wind-blown sand and its control along Qinghai-Tibet Railway in China. Aeolian Research 1, 143. doi:10.1016/j.aeolia.2009.10.001.

Zingg, A.W., 1953. Wind tunnel studies of the movement of sedimentary material, in: Proceedings of the 5th Hydraulic Conference Bulletin, Inst. of Hydraulics, Iowa City. pp. 111–135.

Zio, E., Pedroni, N., 2013. Literature review of methods for representing uncertainty. Foundation for an Industrial Safety Culture.

Zobeck, T.M., Sterk, G., Funk, R., Rajot, J.L., Stout, J.E., Van Pelt, R.S., 2003. Measurement and data analysis methods for field-scale wind erosion studies and model validation. Earth Surface Processes and Landforms 28, 1163–1188. doi:10.1002/esp.1033.